Vehicle handling improvement by fuzzy explicit nonlinear tire forces parametrization

Said Mammar, Andre Benine-Neto, Sebastien Glaser, Naima Ait Oufroukh

Vehicle Handling Improvement by Fuzzy Explicit Nonlinear Tire Forces Parametrization

Saïd Mammar, André Benine-Neto, Sébastien Glaser, Naïma Ait Oufroukh

Abstract— **This paper presents the design and the simulation test of a Takagi-Sugeno (TS) fuzzy output feedback for yaw motion control. The control synthesis is conducted on a nonlinear model in which tire-road interactions are modeled using Pacejka's magic formula. Using sector approximation, a TS fuzzy model is obtained. It is able to handle explicitly the nonlinear Pacejka lateral tire forces including the decreasing or saturated region. The controller acts through the steering of the front wheels and the differential braking torque generation. The computation of the controller takes into account the constraints that the trajectories of the controlled vehicle remain inside an invariant set. This is achieved using quadratic boundedness theory and Lyapunov stability. Some design parameters can be adjusted to handle the trade-off between safety constraints and comfort specifications. The solution to the associated problem is obtained using Linear and Bilinear Matrix Inequalities (LMI-BMI) methods. Simulation tests show the controlled car is able to well achieve standard maneuvers such as the ISO3888-2 transient maneuver and the sine with dwell maneuver.**

Index Terms— **Vehicle handling, Fuzzy control, Output feedback, LMI, BMI.**

I. Introduction

Ground vehicles experience instabilities that are difficult for the driver to control. In fact, bifurcation analysis have shown that the stability region, given for example in the sideslip angle - yaw rate phase plane is limited [1]. In addition its size is function of the driver input on the steering speed, the road adhesion and the longitudinal speed. Notice that instabilities are mainly due to lateral tire-road forces saturation. It is thus important de help the driver in maintaining control of the vehicle is extreme dynamics and even prevent that the vehicle enters them.

In this context, electronic stability control systems (ESC) is the subject of intense research while solutions are already available and become more and more popular on commercial vehicles in Europe. They have largely contributed during the last decade to accident and death reduction [12]. Today's systems act on the vehicle lateral dynamics mainly through independent wheel braking. Recent studies have demonstrated that differential braking may have a better effect on yaw dynamics than independent active wheel braking [13], [14]. Optimal strategies for braking forces allocation have been explored in [15]. In parallel, vehicle handling has been also investigated through active steering [5], [7]. Even if the mechanical linkage between them is still a limiting factor, solutions have been already implemented in series production [17]. In such systems, the additional steering angle is limited and it is expected that real gain from active steering will come with steer-by-wire systems which will offer additional freedom-factors for the controller intervention [16].

Using both steering angle rate and differential braking, this paper proposes a dynamic fuzzy output feedback. The Takagi-Sugeno [8] fuzzy formalism allows modeling of the nonlinear behavior of the lateral forces described by the pacejka formula [6]. The nonlinearity includes the decreasing region. The dynamic output feedback formulation considered in this paper presents three main advantages: the use of only the yaw rate and the steering angle as controller input, better flexibility to formulate the stabilization conditions and the ability to handle input or state constraints and bounded disturbances. This controller uses the property of quadratic boundedness and invariant set [4]. This allows the constraints that the trajectories of the controlled vehicle remain inside an invariant set. In fact, during control intervention, it is important to ensure a good safety level by bounding state variables. The chosen strategy fulfills this requirement and consists of building an invariant set for the system state. It guarantees that each trajectory that starts in the invariant set will not exceed it, hence the trajectories will be bounded inside it [9]. Some design parameters can be adjusted to handle the trade-off between safety constraints and comfort specifications. The solution to the associated problem obtained using Linear and Bilinear Matrix Inequalities (LMI-BMI) methods.

The paper is organized as follows: the next Section gives a description of the developed vehicle lateral dynamics Takagi-Sugeno model of the vehicle. The fuzzy output feedback synthesis, including the requirements concerning the quadratic boundedness, the state constraints and control limitation are then presented in Section 3. In Section 4, simulation results for the ISO 3888-2 and the sine with dwell transient maneuvers which excite the nonlinear tire dynamics are provided. The conclusions wrap up the paper.

II. Vehicle Lateral Dynamics T-S Model

As lateral control is concerned, a simple nonlinear model of a vehicle is obtained by neglecting the roll and pitch motions. This model includes the lateral translational motion and the yaw motion (Fig. 1). The two wheels of each axle are lumped into one located at its center. This leads to the vehicle bicycle model. The lateral forces between each tire

S. Mammar and N. Ait Oufroukh are with Université d'Évry Val d'Essonne, France. IBISC: Informatique, Biologie Intégrative et Systèmes Complexes - EA 4526, 40 rue du Pelvoux CE1455, 91020, Evry, Cedex, France, (e-mail: naima.aitoufroukh, said.mammar@iup.univ-evry.fr).

A. Benine-Neto and S. Glaser are with IFSTTAR - LIVIC Laboratoire sur les Interactions Véhicule-Infrastructure-Conducteur. 14, route de la Minière, Bât 824, 78000, Versailles, France, e-mail: (sebastien.glaser, andre.benine-neto@ifsttar.fr).

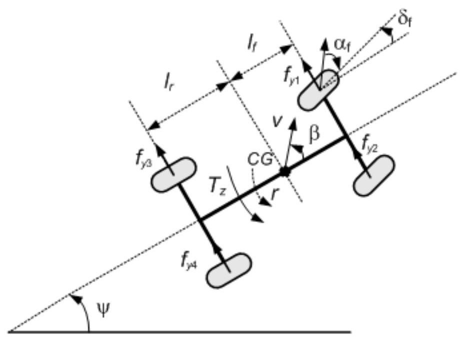

Fig. 1. Vehicle model.

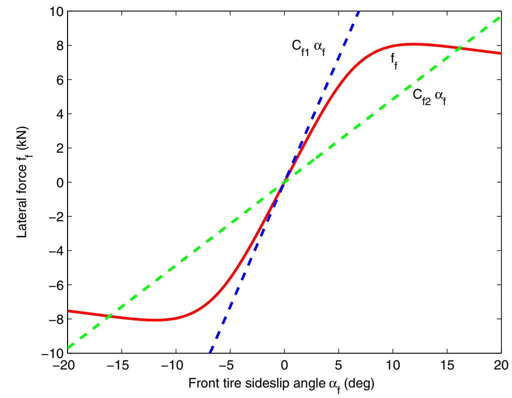

Fig. 2. Tire lateral force given by the pacejka model and sector based approximation.

and the road surface are added at each axle leading to two resulting forces $f_f(\alpha_f) = f_{y1} + f_{y2}$ and $f_r(\alpha_r) = f_{y3} + f_{y4}$ at the front and rear wheels of the bicycle model respectively. These forces which will be detailed below are function of the front and rear tires sideslip angle, denoted α_f and α_r respectively.

The lateral translation and rotational yaw motion equations written in the vehicle fixed frame take the following form

$$\begin{bmatrix} mv\left(\dot{\beta}+r\right) \\ J\dot{r} \end{bmatrix} = \begin{bmatrix} 1 & 1 & 0 \\ l_f & -l_r & 1 \end{bmatrix} \begin{bmatrix} f_f(\alpha_f) \\ f_r(\alpha_r) \\ T_z \end{bmatrix} \tag{1}$$

where β is the vehicle side slip angle, $\dot{\psi} = r$ is the yaw rate and T_z is the yaw moment input applied by differential wheel braking. m is the vehicle mass while J is the vehicle moment of inertia. The vehicle center of gravity is located at a distance l_f from the front axle and a distance l_r from the rear axle. The vehicle parameters values are listed in Table I in the Appendix.

Assuming that the angles remain small, the front and the rear sideslip angles are given by:

$$\begin{aligned} \alpha_f &= \delta_f - \left(\beta + \tfrac{l_f}{v} r\right) \\ \alpha_r &= -\beta + \tfrac{l_r}{v} r \end{aligned} \tag{2}$$

A. Lateral tire forces model

Several types of models of the forces of tire-pavement interaction have been proposed in the literature [6]. They are usually derived from experimental data, as for the Pacejka model, and have as parameters the adhesion, the speed v and the vertical load f_{ni}. The shape of the lateral force is often similar from one model to another. A first linear domain for small sideslip angle allows to define a slope factor called the tire cornering stiffness coefficient. When the sideslip angle increases, the tire enters a nonlinear operating zone where the lateral force saturates. The maximum value defines the limit of the vehicle maneuverability, resulting in a loss of controllability that can cause an understeering phenomenon or an unusual oversteering which may surprise the driver.

Here, the Pacejka magic formula [10], [11] is used to represent the efforts exerted on each tire. This model is based on the mathematical representation of the tire dynamic behavior using analytical functions having a particular structure. Lateral forces of front and rear tires are function of the side slip angle α_i at the tire-road contact location. The effect of the camber angle is neglected. Here, the index i stands for f (front) or r (rear) :

$$\begin{aligned} &f_i(\alpha_i) = \\ &d_i \sin\left(c_i \cdot \tan^{-1}(b_i(1-e_i)\alpha_i + e_i \cdot tan^{-1}(b_i\alpha_i))\right) \end{aligned} \tag{3}$$

Notice that the adhesion coefficient and the normal force acting on each tire are embedded inside the parameters b_i, c_i, d_i and e_i. See [7] for further details. The definition and the value of the above parameters are described in the appendix at the end of the paper.

The goal now is to achieve a Takagi-Sugeno fuzzy model which covers the entire operating domain (linear and non-linear) of the forces [2].

B. Four rules Takagi-Sugeno vehicle fuzzy model

The nonlinear vehicle model is transformed into a four rules Takagi-Sugeno (T-S) fuzzy model according to the values of the front and rear cornering stiffnesses:

- if $|\alpha_f|$ is m_1 and $|\alpha_r|$ is n_1 then $\begin{cases} f_f = c_{f_1}\alpha_f \\ f_r = c_{r_1}\alpha_r \end{cases}$
- if $|\alpha_f|$ is m_2 and $|\alpha_r|$ is n_1 then $\begin{cases} f_f = c_{f_2}\alpha_f \\ f_r = c_{r_1}\alpha_r \end{cases}$
- if $|\alpha_f|$ is m_1 and $|\alpha_r|$ is n_2 then $\begin{cases} f_f = c_{f_1}\alpha_f \\ f_r = c_{r_2}\alpha_r \end{cases}$
- if $|\alpha_f|$ is m_2 and $|\alpha_r|$ is n_2 then $\begin{cases} f_f = c_{f_2}\alpha_f \\ f_r = c_{r_2}\alpha_r \end{cases}$

The membership functions m_i and n_i $(i = 1,2)$ are determined by the approximation method of nonlinear function by linear sectors. Coefficients c_{f_i} and c_{r_i} $(i = 1,2)$ represent the tire cornering stiffnesses associated to each sector. In fact they represent also the slope of the limits of the sectors which include the tire forces (Fig. 2). For example, given two coefficients c_{f_1} and c_{f_2}, chosen according to the expected road adhesion and driving conditions, one can determine the membership functions $m_1(\alpha_f)$ and $m_2(\alpha_f)$. The evolution of the two functions m_1 and m_2 as functions of the sideslip angle are shown in Figure 3. They are obtained with numerical values: $c_{f_1} = 1.2c_f$ and $c_{f_2} = 0.6c_f$. It is important to outline that this sector representation is an exact approximation of the nonlinear system.

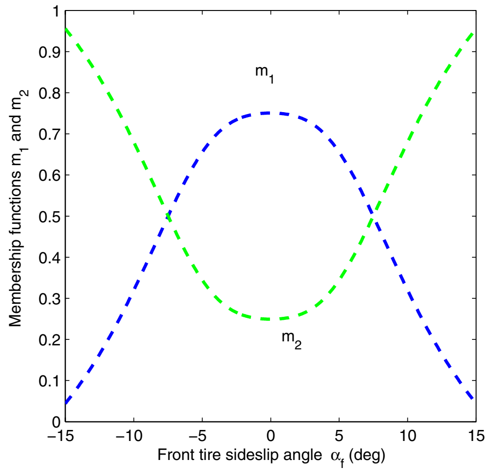

Fig. 3. Membership functions m_1 and m_2 associated to the front tire contact forces.

The membership functions n_1 and n_2 for the rear tire forces are obtained by the same procedure. Finally, one can write:

$$\begin{cases} f_f = \left[(h_1+h_3)c_{f_1} + (h_2+h_4)c_{f_2}\right]\alpha_f \\ f_r = \left[(h_1+h_2)c_{r_1} + (h_3+h_4)c_{r_2}\right]\alpha_r \end{cases} \tag{4}$$

with $h_1 = m_1 \times n_1$, $h_2 = m_2 \times n_1$, $h_3 = m_1 \times n_2$ and $h_4 = m_2 \times n_2$.

In order to have the front and the rear sideslip angle as state vector components, let us define the state $\bar{x} = [\alpha_f, \alpha_r, \delta_f]^T$ and the control input $u = [\dot{\delta}_f, T_z]^T$, the fuzzy system takes the form:

$$\dot{\bar{x}} = \sum_{i=1}^{4} h_i(\alpha_f, \alpha_r)\bar{A}_i\bar{x} + \bar{B}u \tag{5}$$

where

$$\bar{A}_i = \begin{bmatrix} a_{11i} & a_{12i} & a_{13} \\ a_{21i} & a_{22i} & a_{23} \\ 0 & 0 & 0 \end{bmatrix}, \bar{B} = \begin{bmatrix} 1 & -\frac{l_f}{Jv} \\ 0 & \frac{l_r}{Jv} \\ 1 & 0 \end{bmatrix} \tag{6}$$

where

$$\begin{cases} a_{11i} = -\frac{v}{l_f+l_r} - \frac{1}{v}\left(\frac{1}{m} + \frac{l_r l_f}{J}\right)c'_{fi}, \\ a_{12i} = \frac{v}{l_f+l_r} - \frac{1}{v}\left(\frac{1}{m} - \frac{l_f l_r}{J}\right)c'_{r_i}, \\ a_{21i} = -\frac{v}{l_f+l_r} - \frac{1}{v}\left(\frac{1}{m} - \frac{l_r^2}{J}\right)c'_{fi}, \\ a_{22i} = \frac{v}{l_f+l_r} - \frac{1}{v}\left(\frac{1}{m} + \frac{l_r^2}{J}\right)c'_{r_i}, \\ a_{13} = \frac{v}{l_f+l_r}, \\ a_{23} = \frac{v}{l_f+l_r}. \end{cases}$$

where $c'_{fi} = c_{f1}$ for $i = 1,3$ and $c'_{fi} = c_{f2}$ for $i = 2,4$. Similarly, $c'_{ri} = c_{r1}$ for $i = 1,2$ and $c'_{ri} = c_{r2}$ for $i = 3,4$.

C. Reference yaw rate tracking

Ideally, the vehicle should respond to driver's steering angle δ_d as a speed depended yaw rate reference steady state value with almost constant settling time. Let T_0 be the desired transfer function between δ_d and r. In order to ensure at nominal speed, the same steady state value for the controlled and the conventional car, the reference model is chosen as a first order transfer function with the same steady state gain as the conventional car. It is of the form $r_d = \frac{K_d(v)}{\tau s+1}\delta_d$. The speed dependent steady state gain is $K_d(v)$, derived from the nominal linear bicycle model, and $\tau = 0.2$ sec.

In order to ensure that the yaw rate reference value is achieved in steady state, the integral z of the yaw rate tracking error is added as state a variable:

$$\dot{z} = r - r_d = \frac{\delta_f + \alpha_r - \alpha_f}{l_f + l_r}v - r_d \tag{7}$$

This variable is thus added to the previous third order model while the desired yaw rate is considered as a disturbance. The fuzzy model is finally discretized at a sample time of $T = 0.005$ sec. The final fuzzy model is of the form:

$$\begin{array}{l} x(t+1) = \sum_{i=1}^{4} h_i(\alpha_f, \alpha_r)A_i x(t) + Bu(t) + Ew(t) \\ y(t) = Cx(t) + Dw(t) \end{array} \tag{8}$$

where $x = [\alpha_f, \alpha_r, \delta_f, z]^T$ and $y(t) = [r, z]^T$. The disturbance $w(t) = r_d(t) \in \varepsilon_Q = \left\{w \in \mathscr{R}/w^T Q w \leq 1\right\}$ is bounded. Matrices A_i and B can be easily derived from equations (6) and (7). This discrete time fuzzy system is characterized by common B, E and C matrices. This property simplifies drastically the stability and performance conditions as only simple summations are involved.

III. Dynamic output feedback fuzzy controller

In the following, a dynamic output feedback fuzzy controller is sought. It has the form:

$$\begin{array}{l} x_c(t+1) = \sum_{i=1}^{4} h_i(\alpha_f, \alpha_r)A_c^i x_c(t) + B_c y(t) \\ u(t) = C_c x_c(t) + D_c y(t) \end{array} \tag{9}$$

where $x_c \in \mathscr{R}^4$ is the controller state; $\{A_c^i, B_c, C_c, D_c\}$ are matrices to be designed.

This controller uses the parallel distributed compensation (PDC) concept of the fuzzy system control. In this concept, each control rule is distributively designed for the corresponding rule of a T-S fuzzy model. Linear control theory can then be used to design controllers for each of the consequent part of the fuzzy system while ensuring the same properties for the fuzzy system.

As pointed out in [4], D_c is an important parameter for stabilization, and the controller structure is able to handle constraints on the input and the state. By combining (8) and (9), the augmented closed-loop fuzzy model is given by

$$\tilde{x}(t+1) = \sum_{i=1}^{4} h_i(\alpha_f, \alpha_r)\Phi_i\tilde{x}(t) + \Gamma w(t). \tag{10}$$

where $\tilde{x} = \begin{bmatrix} x \\ x_c \end{bmatrix}$, $\Phi_i = \begin{bmatrix} A_i + BD_cC & BC_c \\ B_cC & A_c^i \end{bmatrix}$ and $\Gamma = \begin{bmatrix} BD_cD + E \\ B_cD \end{bmatrix}$.

Let $\Phi_z = \sum_{i=1}^4 h_i(\alpha_f, \alpha_r)\Phi_i$, the closed loop system takes the form: $\tilde{x}(t+1) = \Phi_z\tilde{x}(t) + \Gamma w(t)$.

A. Invariant set and output feedback PDC control

Assume that there exists a quadratic function $V(\tilde{x}) = \tilde{x}^T P\tilde{x}$, where P is a symmetric, positive definite matrix that satisfies, for all $\tilde{x}$, w satisfying (10), $w^TQw \leq 1$, $V(\tilde{x}) \geq 1$, the condition [3]:

$$V(\tilde{x}+1) \leq V(\tilde{x}) \tag{11}$$

Consider the reachable set Λ defined by:

$$\begin{aligned}\Lambda \triangleq \quad & \{\tilde{x}(T)|\tilde{x}, w \text{ satisfying (10)}, \\ & \tilde{x}(0) = 0, w^TQw \leq 1, T \geq 0\}\end{aligned} \tag{12}$$

The set ε_P defined by:

$$\varepsilon_P = \{\tilde{x}(t) \in \mathscr{R}^8 | \tilde{x}(t)^T P\tilde{x}(t) \leq 1\}, \tag{13}$$

is an invariant set for the system (10) with $w \in \mathscr{R}$, $w^TQw \leq 1$. This means that every trajectory that starts inside ε_P remains inside it for $t \to \infty$.

The existence of such a function $V(\tilde{x})$ means that the set ε_P is an outer approximation of the reachable set Λ.

ε_P is also and outer approximation of the reachable set

$$\begin{aligned}\Lambda^* \triangleq \quad & \{\tilde{x}(T)|\tilde{x}, w \text{ satisfying equation (10)}, \\ & \tilde{x}(0) \in \varepsilon_P, w^TQw \leq 1, T \geq 0\}\end{aligned} \tag{14}$$

In this section the control law and the invariant set ε_P are synthesized. This is achieved using BMI (Bilinear Matrix Inequalities) optimization method such that the system without the disturbance is asymptotically stable and at the same time, the reachable set for an initial state values inside the invariant set is contained in this invariant set.

B. Invariant set - quadratic boundedness

According to the previous considerations, the closed loop linear system $\tilde{x}(t+1) = \Phi_z\tilde{x}(t) + \Gamma w(t)$ is strictly quadratically bounded with a common Lyapunov matrix $P > 0$ for all allowable $w(t) \in \varepsilon_Q$, for $t > 0$, if $\tilde{x}(t)^T P\tilde{x}(t) > 1$ implies $(\Phi_z\tilde{x}(t) + \Gamma w(t))^T P (\Phi_z\tilde{x}(t) + \Gamma w(t)) < \tilde{x}^T P\tilde{x}$, for any $w \in \varepsilon_Q$.

The corresponding condition is obtained using the $S-$procedure and invoking the Schur complement, using that the satisfaction of $w \in \varepsilon_Q$ and $\tilde{x}^T P\tilde{x} \geq 1$ implies $w^TQw \leq \tilde{x}^T P\tilde{x}$.

Defining $P = \begin{bmatrix} P_1 & P_2^T \\ P_2 & P_3 \end{bmatrix}$ and $P^{-1} = \begin{bmatrix} M_1 & M_2^T \\ M_2 & M_3 \end{bmatrix}$. Assuming that P_2 and M_2 are full rank matrices and setting:

$$\begin{cases} \hat{D}_c = D_c \\ \hat{C}_c = D_cCM_1 + C_cM_2 \\ \hat{B}_c = P_1BD_c + P_2^TB_c \\ \hat{A}_c^i = P_1A_iM_1 + P_1BD_cCM_1 + P_2^TB_cCM_1 \\ +P_1BC_cM_2 + P_2^TA_c^iM_2 \end{cases} \tag{15}$$

the existence of the controller is ensured if there exist matrices P_1, P_2, M_1, M_2 and a positive scalar α such that the following condition holds

$$\sum_{i=1}^4 h_i(\alpha_f, \alpha_r)\Upsilon_i \geq 0 \tag{16}$$

where

$$\Upsilon_i = \begin{bmatrix} (1-\alpha)P_1 & * & * & * & * \\ (1-\alpha)I & (1-\alpha)M_1 & * & * & * \\ 0 & 0 & \alpha Q & * & * \\ A_i + B\hat{D}_cC & A_iM_1 + B\hat{C}_c & B\hat{D}_cD + E & M_1 & * \\ P_1A_i + \hat{B}_cC & \hat{A}_c^i & \hat{B}_cD + P_1E & I & P_1 \end{bmatrix} \tag{17}$$

Notice that the matrices M_1, M_2, P_1 and P_2 verify:

$$M_2^TP_2 = I - M_1P_1 \tag{18}$$

In addition, it is possible to handle constraints on the control signal and the state:

$$-\bar{u} \leq u(t) \leq \bar{u}, \quad -\bar{\Psi} \leq \Psi x(t+1) \leq \bar{\Psi}, \quad \forall t \geq 0 \tag{19}$$

where $\bar{u} = [\bar{u}_1, \bar{u}_2]^T$ with $\bar{u}_1 > 0$, $\bar{u}_2 > 0$ and $\bar{\Psi} := [\bar{\Psi}_1, \ldots, \bar{\Psi}_q]^T$ with $\bar{\Psi}_j > 0$, $j = 1, \ldots, q$, $\Psi \in \mathscr{R}^{q\times 4}$ and q is the number of imposed constraints. Notice that the bounds are provided separately on each state variables or a combination of state variables.

The control input limitation is verified if for a pre-specified scalar $\eta \in (0, 1]$, the additional inequality

$$\begin{bmatrix} \eta P_1 & * & * & * \\ \eta I & \eta M_1 & * & * \\ 0 & 0 & Q & * \\ \sqrt{2}\hat{D}_cC & \sqrt{2}\hat{C}_c & \sqrt{2}\hat{D}_cD & Z \end{bmatrix} \geq 0 \tag{20}$$

holds with $Z \in \mathscr{R}^{2\times 2}$ is such that $Z_{11} \leq \bar{u}_1^2$ and $Z_{22} \leq \bar{u}_1^2$.

A similar procedure can be applied for the constraints on the state variables. One can achieve from the convex property conditions (21):

$$\begin{array}{ll} \sum_{i=1}^4 h_i(\alpha_f, \alpha_r)\widetilde{\Upsilon}_i \geq 0, & t \geq 0, \\ \Xi_{kk} \leq \bar{\Psi}_k^2, & k \in \{1, \ldots, q\} \end{array} \tag{21}$$

where Ξ is a symmetric matrix and

$$\widetilde{\Upsilon}_i = \begin{bmatrix} \eta P_1 & * & * & * \\ \eta I & \eta M_1 & * & * \\ 0 & 0 & Q & * \\ \widetilde{\Upsilon}_{i41} & \widetilde{\Upsilon}_{i42} & \widetilde{\Upsilon}_{i43} & \Xi \end{bmatrix} \tag{22}$$

and

$$\begin{aligned} \widetilde{\Upsilon}_{i_{41}} &= \sqrt{2}\Psi(A_i + B\hat{D}_cC) \\ \widetilde{\Upsilon}_{i_{42}} &= \sqrt{2}\Psi(A_iM_1 + B\hat{C}_c) \\ \widetilde{\Upsilon}_{i_{43}} &= \sqrt{2}\Psi(B\hat{D}_cE + D) \end{aligned}$$

C. Controller synthesis

Under the proposed modeling approach, the desired yaw rate could be seen as an input disturbance under which the closed-loop system should remain stable with bounded values for the state vector components. More generally, the state variables should not exceed the bounds of a "safety zone", namely $\left|\alpha_f\right| \leq \alpha_f^M$, $|\alpha_r| \leq \alpha_r^M$ and $\left|\delta_f\right| \leq \delta_f^M$. Thus, the state vector x has to be confined to a hypercube $L(Z^M)$ defined by the above bounds. Finally, the control input, the steering angle rate and the yaw moment, have to be bounded $\left|\dot{\delta}_f\right| \leq \dot{\delta}_f^M$ and $|T_z| \leq T_z^M$.

According to the equation (19), control limitation is given by $\bar{u} = [\dot{\delta}_f^M, T_z^M]$, while state limitation is given by $\bar{\Psi} = [\alpha_f^M, \alpha_r^M, \dot{\delta}_f^M]^T$ and $\Psi = \left[\begin{array}{cc} I_3 & 0 \end{array}\right]$.

The PDC output feedback controller was synthesized with the following numerical values:

$$\begin{array}{lll} \alpha = 0.02, & \eta = 0.02, & \dot{\delta}_f^M = 100\,\mathrm{deg}/s, \\ T_z^M = 10KN & \alpha_f^M = \alpha_r^M = 13\,\mathrm{deg} & \delta_f^M = 6\,\mathrm{deg}, \end{array}$$

These design parameters could be adjusted to handle the trade-off between safety constraints and comfort specifications.

The achieved Q is 5, which ensures that the constraints are verified for a disturbance of a magnitude less than $0.447 rad/s$ at the considered longitudinal speed of $20 m/s$. In fact, the maximum value is constrained by [18]:

$$r_{d_{\max}} = 0.85 \frac{g}{v}$$

.

IV. Simulation tests

In order to proof the assistance ability to maintain the dynamic vehicle stability in extreme conditions, several type of maneuvers have been defined to test the ESC systems. Among them, double lane-change manoeuvre defined in ISO 3888-2 standard and the sine with dwell transient maneuver. The controller is tested below for the two maneuvers.

A. Testing for the ISO 3888-2 maneuver

The ISO3888-2 double lane-change maneuver setup is depicted in Figure 4-a. The maneuver is carried out with and without the controller at the same speed of $80 km/h$. During the maneuver, the throttle is released.

The driver initiates the maneuver by applying the steering angle shown in dashed line in Figure 4-b. Figures 4-a highlights that the controlled vehicle is able to perform the maneuver (solid line) while the uncontrolled vehicle fails (dashed line). Figure 4-d shows that the controller shares the effort on the steering angle rate an the yaw moment, respectively. In this situation the driver applied steering angle is too high (dashed line in Figure 4-b) while the the steering angle of the controlled vehicle is limited to the admissible safety value of few degrees, as shown by the solid line in Figure 4-b for the angle value. The steering angle rate is depicted in the top plot of Figure 4-d and is limited. The the yaw moment handles the main effort as shown in the bottom

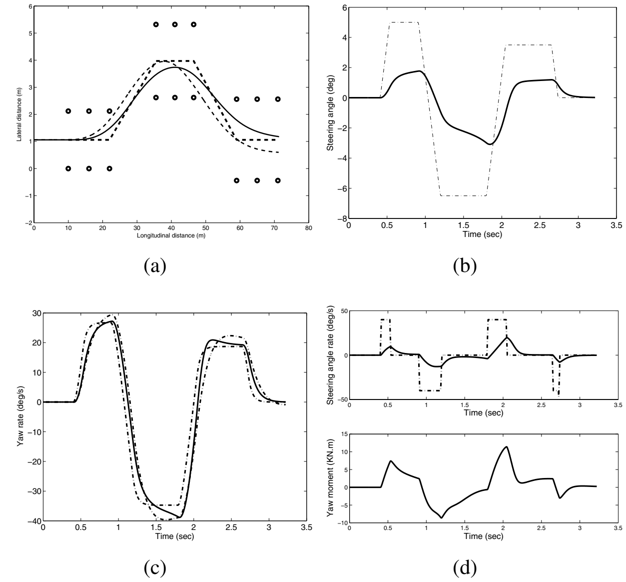

Fig. 4. ISO3888-2 maneuver: Yaw rate, steering angle, steering angle rate and trajectory for the uncontrolled and the controlled vehicles.

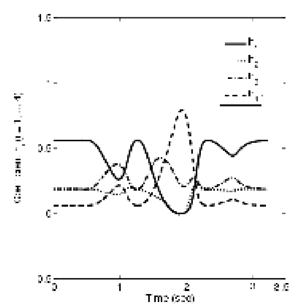

Fig. 5. ISO3888-2 maneuver: Coefficients h_i reflecting the contribution of each sub-controller for the controlled vehicles.

plot of Figure 4-d. Figure 4-c shows that the controlled car yaw rate is closer to the reference one than the yaw rate of the uncontrolled vehicle (dashed line). The contribution of each sub-controller to according to the actual vehicle dynamics are shown in Figure 5. Finally, Figures 6-a and 6-b provide the developed sideslip angles at the front and rear tires. The corresponding front and rear forces are shown in Figures 6-c and 6-d. It is clear that the saturation zones are reached by the uncontrolled vehicle during the maneuver while the controller avoids that these zones are reached.

B. Sine with dwell maneuver

The sine with dwell is a transient maneuver considered by NHTSA (National Highway Traffic Safety Administration) for electronic stability control evaluation. Such type of maneuver is suited for the excitation of the vehicle oversteer response. The maneuver is conducted at the same speed of 80km/h. It corresponds to a 0.7Hz frequency sine wave form with dwell steering angle of 500ms. During the maneuver, the throttle is released. Figure 7 shows both the control sharing

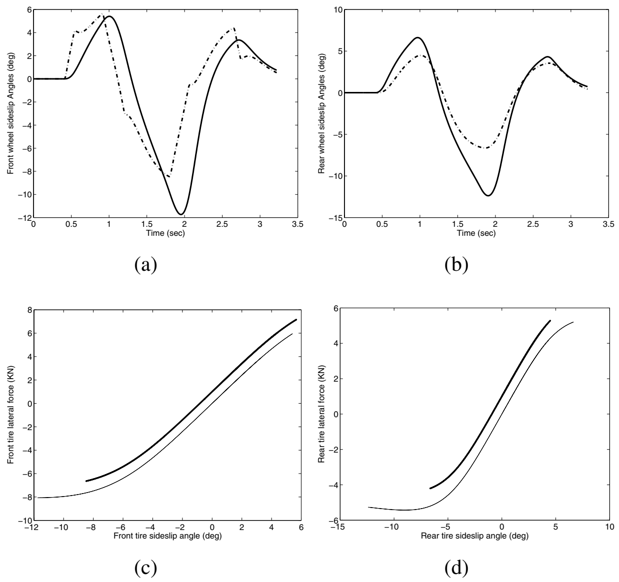

Fig. 6. ISO3888-2 maneuver: Front and rear tire sideslip angle and corresponding lateral forces for the uncontrolled (dashed) and the controlled vehicles (solid), with vertical offset for the uncontrolled one for better display.

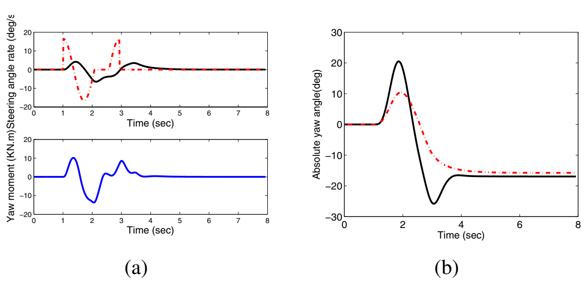

Fig. 7. Sine with dwell maneuver: Steering rate and differential braking control inputs, vehicle absolute yaw angle. Dashed line for the uncontrolled vehicle and solid line for the controlled one.

between the steering and the differential braking. It also shows that the realized relative yaw angle is higher which means that the vehicle is more able to change direction.

V. Conclusion

In this paper the design and the test of an integrated steering and differential braking control for yaw moment generation has been described. Controlled vehicle trajectories are confined inside an invariant set. The nonlinear behavior of the vehicle dynamics are modeled using a fuzzy Takagi-Sugeno approach. An output feedback fuzzy controller constituted by four sub-controllers handles constraints on the state variables and the control inputs. Simulation tests have shown that the controlled vehicle is able to achieve the ISO 3888-2 and the sine with dwell transient maneuvers where the uncontrolled vehicle fails.

Appendix

TABLE I

Vehicle parameters.

m	Vehicle total mass 1600 kg.
c_f	Front cornering stiffness 40000 N/rad.
c_r	Rear cornering stiffness 35000 N/rad.
J	Vehicle yaw moment of inertia 2454 kg$\cdot m^2$.
l_f	Distance form CG to front axle 1.22m.
l_r	Distance from CG to rear axle 1.44m.
v	Longitudinal velocity.

TABLE II

Tire model parameters.

Tire	b_i	c_i	d_i	e_i
Front $(i=f)$	8.3278	1.1009	4536.0	-1.661
Rear $(i=r)$	11.6590	1.1009	3671.6	-1.542

References

[1] H.D. Tuan, E. Ono, S. Hosoe, S. Doi, Bifurcation in Vehicle Dynamics and Robust Front Wheel Steering Control. IEEE Transactions on Control Systems Technology, 6, pp. 412-421, 1998.

[2] T. Takagi, M. Sugeno, Fuzzy identification of systems and its application to modeling and control, IEEE Trans. Systems Man Cybern. 15, pp. 116-132, 1985.

[3] A. Alessandri, M. Baglietto, G. Battistelli, Design of state estimators for uncertain linear systems using quadratic boundedness. Automatica, 42, 497-502, 2006.

[4] B. Ding, Quadratic boundedness via dynamic output feedback for constrained nonlinear systems in Takagi–Sugeno's form, Automatica, vol. 45, N° 9, pp. 2093-2098, 2009.

[5] J. C. Gerdes et E. J. Rossetter A Unified Approach to Driver Assistance Systems Based on Artificial Potential Fields Authors. Journal of Dynamic Systems, Measurement and Control, Vol. 123, No. 3, pp. 431-438, 2001.

[6] E. Bakker, H. B. Pacejka, and L. Lidner. A new tire model with an application in vehicle dynamics studies. SAE paper, 1989.

[7] S. Mammar and D. Koenig, Vehicle Handling improvement by Active Steering, Vehicle Sys. Dyn. Journal, vol 38, No3, pp. 211-242, 2002.

[8] K. Tanaka, H.O. Wang, Fuzzy Control Systems Design and Analysis, Wiley Inc, New York, 2001.

[9] N. Minoiu, M. Netto, S. Mammar, B. Lusetti, Driver steering assistance for lane departure avoidance, Control Engineering Practice, Vol. 17, No 6, pp. 642-651, 2009.

[10] Hans B. Pacejka, *Tyre and Vehicle Dynamics*, p 511- 562 , Delft University of Technology, 2002.

[11] W.D. Versteden, *Improving a tyre model for motorcycle simulations*, Maters Thesis, Technical University of Eindhoven, June 2005.

[12] Grands thèmes de la sécurité routière en France. ONISR, Observatoire national interministériel de sécurité routière, février 2007.

[13] A.T.V. Zanten, R. Erhart, and G. Pfaff, VDC, The Vehicle Dynamics Control System of Bosch, , SAE Technical Paper No. 95759 , 1995.

[14] M.J. Hancock, R.A. Williams, T.J. Gordon, M.C. Best, A comparison of braking and differential control of road vehicle yaw-sideslip dynamics, Proceedings of IMechE., Part D: Automobile Engineering, V.219, pp. 309-327, 2005.

[15] J. Tjoennas and T. A. Johansen, Adaptive Optimizing Dynamic Control Allocation Algorithm for Yaw Stabilization of an Automotive Vehicle using Brakes, in Control and Automation, 2006. MED '06. 14th Mediterranean Conference on, 2006, pp. 1-6.

[16] E. Ono, Y. Hattori, Y. Muragishi, K. Koibushi, Vehicle Dynamics Integrated Control for Four-Wheel-Distributed Steering and Four-Wheel-Distributed Traction/Braking Systems, Vehicle System Dynamics, V.44, No.2, pp. 139-151, 2006.

[17] P. Kohen and M. Ecrick, Active Steering - The BMW Approach Towards Modern Steering Technology, SAE Technical Paper No. 2004-01-1105, 2004.

[18] Rajamani R., Vehicle Dynamics and Control, Springer, New-York, 2006.